MedChemComm

Accepted Manuscript

This article can be cited before page numbers have been issued, to do this please use: N. R. Filipovi, S. Bjelogrli, G. Portalone , S. Pelliccia, R. Silvestri, O. R. Klisuri, M. Senanski, D. M. Stankovi, T. R. Todorovi and C. D. Muller, *Med. Chem. Commun.*, 2016, DOI: 10.1039/C6MD00199H.

ROYAL SOCIETY OF CHEMISTRY

www.rsc.org/medchemcomm

View Article Online
DOI: 10.1039/C6MD00199H

Pro-apoptotic and pro-differentiation induction by 8-quinolinecarboxaldehyde selenosemicarbazone and its Co(III) complex in human cancer cell lines[†]

Nenad R. Filipović,[a] Snežana Bjelogrlić,[b] Gustavo Portalone,[c] Sveva Pelliccia,[d] Romano Silvestri,[d] Olivera Klisurić,[e] Milan Senćanski,[f] Dalibor Stanković,[g] Tamara R. Todorović,[h,*] Christian D. Muller[i,*]

[a]*Faculty of Agriculture, University of Belgrade, Nemanjina 6, Belgrade, Serbia.*

[b]*National Cancer Research Center of Serbia, Pasterova 14, Belgrade, Serbia.*

[c]*Dipartimento di Chimica, Sapienza Universita di Roma, Piazzale Aldo Moro 5, I-00185 Roma, Italy.*

[d] *Dipartimento di Chimica e Tecnologie del Farmaco, Sapienza Universita di Roma, Piazzale Aldo Moro 5, I-00185 Roma, Italy.*

[e]*Department of Physics, Faculty of Sciences, University of Novi Sad, Trg Dositeja Obradovića 4, Novi Sad, Serbia.*

[f]*Center for Multidisciplinary Research, Institute of Nuclear Sciences "Vinča", University of Belgrade, Belgrade, Serbia*

[g]*Innovation Center of the Faculty of Chemistry, University of Belgrade, Studentski trg 12-16, Belgrade, Serbia.*

[h]*Faculty of Chemistry, University of Belgrade, Studentski trg 12-16, Belgrade, Serbia; E-mail: tamarat@chem.bg.ac.rs*

[i]*Institut Pluridisciplinaire Hubert Curien, UMR 7178 CNRS Université de Strasbourg, 67401 Illkirch, France; E-mail: cdmuller@unistra.fr*

Corresponding authors:

Tamara R. Todorović, E-mail: tamarat@chem.bg.ac.rs

Christian D. Muller, E-mail: cdmuller@unistra.fr

[†] The authors declare no competing interests.
Electronic Supplementary Information (ESI) available: The experimental section can be found in the supplementary materials (ESI). NMR (Figs. S1 and S2) and UV-Vis (Fig. S3) spectra; cyclic voltammograms (Fig. S4); packing diagrams (Figs. S5 and S6); sigmoidal dose-response curves (Fig. 7); activity on THP-1 cell line (Figs. S8 and S9); activity on caspase-8 and 9 (Fig. S10); the ligand H8qasesc and complex binding sites of HSA (Fig. S11); crystal data and selected geometrical parameters (Tables S1-S3); Hydrogen bond and π-π stacking interaction parameters (Table S4); interactions of HSA binding site (Table S5). CCDC 1471189 and 1401687. For ESI and crystallographic data in CIF or other electronic format see DOI: xxxxx

View Article Online
DOI: 10.1039/C6MD00199H

Abstract

8-Quinolinecarboxaldehyde selenosemicarbazone (H8qasesc) and its octahedral Co(III) complex were characterized by means of single crystal X-ray diffraction analysis, spectroscopy methods and cyclic voltammetry. Antineoplastic activity of the ligand and the complex has been assessed on acute monocytic leukemia cell line (THP-1) and AsPC-1 cancer stem cell line (CSC) derived from patient suffering pancreatic adenocarcinoma, with cisplatin (CDDP) as a reference compound. Evaluation involved determination of pro-apoptotic activity, changes in cell cycle distribution, role of caspase activation in process of cell death, and ability of investigated compounds to challenge reprogramming of CSC phenotype. Compared to CDDP, treatment with H8qasesc induced higher apoptotic response in both investigated cell lines. Apoptosis triggered by H8qasesc was highly caspase-dependent, but did not include activation of either caspase-8 or -9. According to cell cycle changes H8qasesc delayed transition of cells during DNA replication, but in a manner different than CDDP. The ligand did not show nuclease activity on pUC19 plasmid, while docking studies disclosed that it does not have intercalating properties. Treatment of THP-1 cells with Co(III) complex resulted in strong toxic response, whereas cell death in treated AsPC-1 line was not achieved for 24 h. Additionally, the complex concentration-dependently digested plasmid DNA which might be the cause of its cytotoxic activity. Finally, H8qasesc successfully initiated reprogramming of CSC phenotype in AsPC-1 cell line.

View Article Online
DOI: 10.1039/C6MD00199H

1. INTRODUCTION

Selenosemicarbazones are Schiff bases obtained by condensation reaction of carbonyl compounds and selenosemicarbazides. They showed antiparasitic,[1] antifungal,[2, 3] antibacterial,[3-6] antimalarial,[7-10] anticancer,[3, 7, 10-23] antioxidant[3, 14] and antidiabetic[14] activity. In order to obtain more active species, complexes of Pt(II), Pd(II), Zn(II), Cd(II), Au(I), Ni(II), Co(III), Ga(III), Sn(IV) and Cu(II) have been prepared and tested against malaria,[10, 24, 25] microorganisms,[3-5] as well as cancer cell lines.[3, 11, 16-23, 26] As a result of such approach metal complexes with activities better than corresponding ligands have been developed.[3, 4, 19-23, 26]

Despite the fact that investigation of biological activity of selenosemicarbazones started in the late fifties, apart from our research, up to now there are only three publications where mechanistic studies have been performed.[11, 23, 27] First, Agrawal *et. al.* showed that 5-hydroxy-2-formylpyridine selenosemicarbazone (5HPSe) caused marked inhibition of DNA synthesis *in vitro*, as measured by the incorporation of thymidine-methyl-^{3}H, 5-^{3}H-cytidine or adenine-8-^{14}C into DNA.[11] It was shown that primary target of 5HPSe was ribonucleotide reductase (RR). The recent study underlined the importance of reactive oxygen species (ROS) generation and activation of lysosomal apoptotic pathway through lysosomal membrane permeabilization (LMP) in the anticancer activity of 2-acetylpyridine 4,4-dimethyl-3-selenosemicarbazone and demonstrated lysosomal targeting as a novel mechanism of selenosemicarbazone antiproliferative activity.[27]

Biological properties of 2-formylpyridine selenosemicarbazone, 2-quinolinecarboxaldehyde selenosemicarbazone, 8-quinolinecarboxaldehyde selenosemicarbazone and 2,6-diacetylpyridine bis(selenosemicarbazone) (Hfpsesc, Hqasesc, H8qasesc and H_2dapsesc, respectively, Scheme 1) were systematically examined in our group.[3, 17-20, 26] Monoselenosemicarbazones Hqasesc, Hfpsesc and H8qasesc had ability to act as anti-proliferative agents, inducing apoptosis and cell cycle perturbations in different malignant cell lines, while bis(selenosemicarbazone) H_2dapsesc was far more active against normal than malignant cell lines, predominantly exerting necrotic cell death.[3, 17-20, 26] The ligand Hqasesc induced growth inhibition in several cancer cell lines, although IC_{50} values were 2–10 times higher compared to those of cisplatin (CDDP). Being mostly successful on human cervical adenocarcinoma (HeLa) cells, Hqasesc triggered a significant increase of sub-

View Article Online
DOI: 10.1039/C6MD00199H

G0/G1 cell population as compared to non-treated control that confirmed its ability to trigger apoptotic cell death.[20] This ligand also caused strong concentration dependent apoptosis induction in acute monocytic leukemia (THP-1) cells, while in pancreatic adenocarcinoma cell line (AsPC-1) it induced apoptosis only at the highest concentration.[26] The ligand Hfpsesc was tested on a wide range of malignant cell lines, such as human breast adenocarcinomas (MB-453 and MB-361), human osteosarcoma (U2Os) and its CDDP-resistant sibling U2OS-Pt, HeLa cells, human melanoma (FemX), human colorectal adenocarcinoma (LS174), and murine melanoma (B16).[19] Its activity revealed to be phenotype specific, with stronger inhibition of cell growth than CDDP on MDA-361, LS-174, and B16 cells. In LS174, FemX and MDA-143 cell lines, treatment with Hfpsesc resulted in accumulation of cells in S-to-G2/M phase, while for U2OS and U2OS-Pt cells were accumulated exclusively in the S phase. The ligand H8qasesc showed the same degree of antiproliferative activity against U251 cell line as CDDP, with a 20 times higher antioxidant potential when compared to Vitamin C.[3]

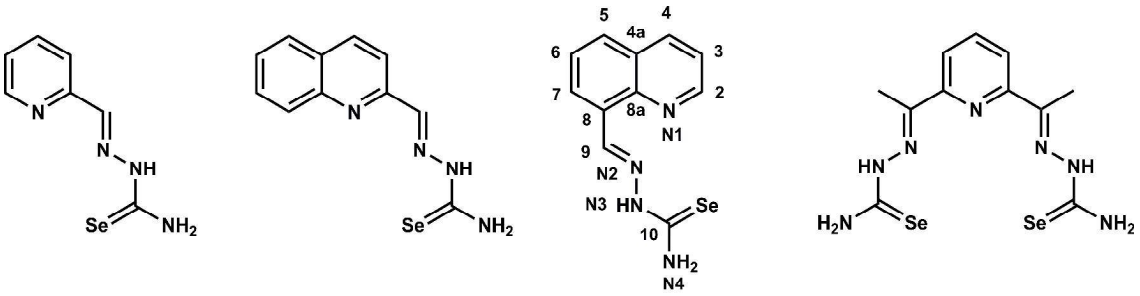

Scheme 1. Structures of mono- and bis(selenosemicarbazone) ligands.

Preparation of Pt(II), Pd(II), Cd(II), Ni(II), Co(III) and Zn(II) complexes with Hqasesc and Hfpsesc, as well as Pt(II) and Pd(II) complexes with H8qasesc resulted in compounds more potent than CDDP and the ligands themselves.[3, 17-20] In general, monoselenosemicarbazone complexes induced apoptosis in all investigated cell lines.[3, 17, 19, 20, 26] In the case of bis selenosemicarbazone ligand H_2dapsesc and its Cd(II) and Zn(II) complexes, neither caspase activity nor ROS production were induced in treated cells.[18] More detailed mechanistic analysis of the action of Cd complex of Hqasesc revealed that it causes

View Article Online
DOI: 10.1039/C6MD00199H

cell cycle arrest in G0/G1 stage, massive caspases activation and production of ROS.[3] The Zn(II) complex of Hqasesc interfered with DNA replication causing concentration-dependent apoptotic induction in THP-1 cells, which coincided with an arrest at the S phase of mitotic division.[26] On the other hand, dramatically increased phosphorylation of extracellular receptor kinase, with recorded release of cytochrome C and activation of p73 in HeLa and MDA-361 cells treated with Hfpsesc and its Cd(II), Ni(II) and Zn(II) complexes, were detected.[17] Ni(II) complex with Hfpsesc also showed potent anti-metastatic activity.[16] Our studies have pointed out the importance of the nature of the metal ions in the mechanism of activity of selenosemicarbazone complexes.

Cobalt is particularly suitable for complexation with selenosemicarbazones since it is biometal and already serves as co-factor in a number of natural enzymes.[28, 29] In our previous work we synthesized Co(III) complex with Hqasesc ligand, $[Co(qasesc)_2]BF_4$, which did not show promising anticancer activity.[19] In this complex, the ligand Hqasesc was tridentately (NNSe) coordinated, with the formation of two 5-membered chelate rings. Here we present the synthesis and characterization of a novel Co(III) complex with H8qasesc ligand, structural isomer of Hqasesc. Two isomers have the same mode of coordination, but H8qasesc is capable to form one 5-membered and 6-membered chelate rings. Our recent report indicates that chelate ring size may induce difference in biological activity of metal complexes.[30]

In the current study, evaluation of anticancer potency of H8qasesc and its Co(III) complex was managed in order to investigate their pro-apoptotic activity on two malignant cell lines with pro-differentiation activity on cancer stem cells (CSCs). The human pancreatic adenocarcinoma AsPC-1 is expressing epithelial-masenchymal transition (EMT)-associated genes which promote tumor progression and metastasis, and designate this cell line as a good cancer stem cell model.[31] CSCs are rare immortal cells within a tumor, dividing rapidly unlike stem cells of healthy tissues, and giving rise to resistance to therapy and tumor relapse.[32] Results from experimental models and clinical studies showed that CSCs survive many commonly employed cancer treatments, giving them a high clinical relevance. Elimination of CSCs is set as the crucial need in intention to cure the cancer. For these reason, together with THP-1 cell line, we challenged our compounds against AsPC-1 cell line to evaluate their ability either to trigger apoptotic death and/or induce differentiation.

View Article Online
DOI: 10.1039/C6MD00199H

2. RESULTS & DISCUSSION

2.1. Synthesis and characterization

Cobalt(III) complex with *N*-heteroaromatic selenosemicarbazone ligand H8qasesc has been synthesized. The complex was prepared by template reaction starting from $Co(ClO_4)_2 \times 6H_2O$, 8qa and selenosemicarbazide (mole ratio 1 : 2 : 2, respectively). The complex is soluble in MeOH, EtOH, MeCN, DMF and DMSO at room temperature. Molar conductivity measurements showed that obtained complex is 1 : 1 type of electrolyte. Value of molar conductivity was unchanged after 24 h, indicating that complex is stabile in the solution. Elemental analysis showed that complex contains two deprotonated H8qasesc ligands, one perchlorate anion and one crystalline DMSO molecule. Concerning the all above mentioned, the following formula of novel Co(III) complex could be derived: $[Co(8qasesc)_2]ClO_4 \times DMSO$ (**1**). The complex **1** is diamagnetic in nature which was confirmed by magnetic moment measurement at room temperature. The structure of **1** was elucidated by spectroscopic (IR, NMR and UV-Vis) and crystallographic methods. Since the ligand was obtained as a single-crystalline solid, its structure was determined by crystallographic methods also. Electrochemical behavior of the ligand and **1** was studied by cyclic voltammetry.

In the IR spectrum of **1**, shifts of the ν(C=N) toward higher frequencies (1604 cm^{-1} in H8qasesc and 1615 cm^{-1} in **1**), and ν(C–Se) to lower frequencies (784 cm^{-1} in H8qasesc and 761 cm^{-1} in **1**) was noticed**.** The same frequency shift pattern was found for the ligand Hqasesc and its Co(III) complex, which was indication of coordination of imine nitrogen atom and selenium atom to Co(III).[4] Also, in the IR spectrum of **1** the sharp and strong band at ~ 1068 cm^{-1} originating from perchlorate ion can be observed.

The labeling of atoms in H8qasesc used in NMR is given in Scheme 1. ^{1}H NMR spectrum of **1** (Fig. S1A, ESI) shows that nitrogen atom N3 is deprotonated as evidenced by the absence of the H–N3 signal at 11.98 ppm in ^{1}H NMR spectrum of H8qasesc. Coordination *via* the selenium atom can be seen by the strong upfield shift of C10 signal in ^{13}C NMR spectrum of **1** (Fig. S1B, ESI) in comparison to signal of the same carbon atom in the spectrum of metal-free H8qasesc. Coordination *via* the quinoline nitrogen atom can be observed by the upfield shift of H–C2, and downfield shifts of H–C4 and H–C5 in the ^{1}H NMR spectrum of the complex **1**. There is also an evidence for coordination *via* the quinoline

View Article Online
DOI: 10.1039/C6MD00199H

nitrogen atom in the ^{13}C NMR spectrum, since signals of C2, C4 and C8a are shifted downfield. Coordination *via* the azomethine nitrogen atom can be seen by the strong upfield shift of H–C9 in the ^{1}H NMR spectrum of the complex, and by a downfield shift of C9 signal in the ^{13}C NMR spectrum of the complex. There is also an interesting correlation in the 2D ROESY spectrum of **1** (Fig. S2, ESI), namely H–C2 is correlated with H–C9 and H–C7. This correlation points to the octahedral geometry of the complex, in which these atoms originating from two ligands are in proximity. This indicates that an octahedral geometry of the complex is preserved in the solution.

The electronic spectrum of **1** (Fig. S3A, ESI) exhibits four bands in the region 222–430 nm. Three bands, at 222, 296 and 354 nm, can be assigned to intra ligand $n\rightarrow\pi^*$ transitions of the azomethine portion and $\pi\rightarrow\pi^*$ transitions of the aromatic ring, while band at 422 nm was assigned to the ligand to metal charge transfer transition. The same number of bands and distribution of their intensities was found for similar Co(III) complex with 2-acetylpyridine thiosemicarbazone.[33] The aqueous solution behavior of **1** with respect to hydrolysis was studied in DMSO/H_2O 1:100 (v/v) solution at ambient temperature over 24 h by UV-Vis spectroscopy. The complex **1** was stable, as can be seen from its electronic absorption spectra (Fig. S3B, ESI).

Electrochemical behavior of the ligand H8qasesc and **1** was studied by cyclic voltammetry in the potential range of –2.0 to +1.2 V *vs* Ag/AgCl electrode (Fig. S4, ESI). In the cyclic voltammogram of H8qasesc there are four well defined oxidation peaks at potentials of –0.382, +0.134, +0.48 and +0.994 V. By reduction of H8qasesc three peaks were observed at –0.03, –1.077 and –1.43 V. From these values it could be concluded that almost all observed peaks belong to the irreversible electrochemical reactions, and only redox couple at $E_{1/2}$ = +0.07 V (oxidation at +0.134 V and reduction at –0.03 V) could be attributed to the quasi-reversible electrochemical processes. Under the same experimental conditions, two new well-defined peaks were observed in the cyclic voltammogram of **1**. By comparison of the peak potentials one could conclude that shifts in peak positions can be attributed to the oxidation and reduction of electro-active groups from the ligand. Corresponding reduction peaks at –1.81 and –1.91 V represent reduction of Co(III) to Co(II) and the first oxidation peak at –1.78 V corresponds to the reverse oxidation process. This implies that metal ion from the complex is easy accessible to the electrode surface. All presented results were

View Article Online
DOI: 10.1039/C6MD00199H

obtained after baseline background subtraction, to ensure that the observed peaks belong to the redox behavior of the complex.

2.2. Description of crystal structures

The molecular structures and atom numbering schemes of H8qasesc and **1** are shown in Fig. 1, while Table S1 (ESI) lists the pertinent X-ray crystallographic data for the two compounds. The ligand H8qasesc crystallizes in the monoclinic crystal system and $P2_1/c$ space group, with four molecules in the unit cell. The selected bond lengths and angles for H8qasesc are shown in Table S2 (ESI). The molecule of H8qasesc can be considered as planar, with the highest displacement of N4 nitrogen atom (0.084 Å) from the root mean plane through all non-hydrogen atoms of the ligand. Dihedral angles (Table S3, ESI) confirmed planar geometry of the molecule. The crystal packing is dominated by hydrogen bonds (Fig. S5, ESI).

The cobalt(III) ion coordinates two deprotonated H8qasesc ligands giving the octahedral bischelate cation $[Co(8qaSeC)_2]^+$ with *mer* geometry (Fig. 1B). In the outer sphere of the complex, there is one perchlorate ion and one DMSO solvent molecule. The sulfur atom from the DMSO molecule is disordered over two sites with occupation factors 0.88 and 0.12. Although the complex cation in **1** possesses a chiral octahedral arrangement, overall **1** is racemic compound since it crystallizes in the centric *P*-1 space group. The deprotonated ligand coordinates the metal in a tridentate fashion by means of the selenium atom, the quinoline and the imine nitrogen atoms, forming one six-membered and one five-membered chelate rings with the essentially planar ligand skeleton. The selenium donor atoms deviate slightly from the average planes formed by the ligands' skeleton (0.35 and 0.19 Å respectively for Se1 and Se2). This slight distortion from planarity is due to an intramolecular repulsion between the selenium atoms which are forced by the bischelate coordination to come closer than the sum of their van der Waals radii (Se1…Se2 = 3.358(5) Å, rSe = 1.90Å). All metal-donor atom bonds (Table S2, ESI) are similar to the average corresponding bonds found in a search on quinoline thio/selenosemicarbazone-Co systems performed through the Cambridge Structural Database (CCDC: 734053; 2015 release, v. 5.36 with updates: Nov14, Feb15).[34] The crystal packing of **1** (Fig. S6 and Table S4, ESI) is based on hydrogen bonds involving terminal NH_2 groups, deprotonated hydrazinic nitrogen atom, perchlorate ions and DMSO molecules, as well as π-π stacking interactions of the quinoline rings.

View Article Online
DOI: 10.1039/C6MD00199H

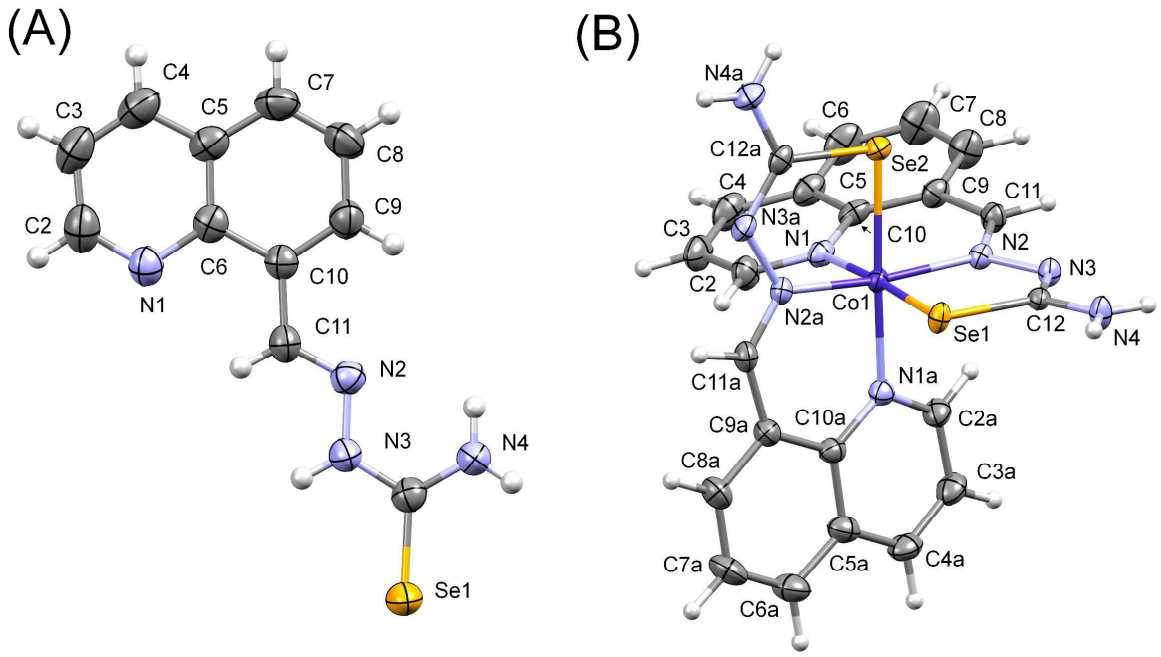

Fig. 1. Molecular structure of H8qasesc (A) and $[Co(8qasesc)_2]^+$ (**1**) (B) with the non-H atom numbering scheme (displacement ellipsoids at 40% probability level).

2.3. Free radical scavenging activity

Because selenium antioxidants can prevent oxidative damage, numerous animal and clinical trials have investigated the ability of these compounds to prevent the oxidative stress, an underlying cause of cancer. Interest in selone (C=Se) antioxidants can be attributed to the naturally occurring selenoneine, a compound that effectively scavenges 1,1-diphenyl-2-picryl-hydrazyl (DPPH) radical.[35] In our previous study we have determined the free radical-scavenging activity of selenosemicarbazones and their metal complexes by ABTS method.[3] Our results showed that H8qasesc is an excellent ABTS cation radical-scavenger, with greater efficacy than Vitamin C. Coordination of the ligand to Pt(II) and Pd(II) canceled antioxidant activity of corresponding complexes.

The proton donating ability of the H8qasesc and **1** was assayed using the DPPH method, a protocol for determination of radical scavenging activity.[36] Ascorbic acid was used as the reference compound (50–500 μg/mL). The results (expressed as IC_{50} in μM: 12.5 for

View Article Online
DOI: 10.1039/C6MD00199H

H8qasesc, 5150 for **1** and 79.3 for Vitamin C) corroborate our previous finding by mean of ABTS method. The ligand H8qasesc has an excellent free radical-scavenging activity, better than the reference molecule Vitamin C. On the other hand, coordination of H8qasesc to Co(III) diminished the activity of corresponding complex.

2.4. H8qasesc stimulated stronger apoptotic response compared to 1 and CDDP

The ability of H8qasesc and **1** to induce death of THP1 and AsPC1 cells was tested in a span of six concentrations after 24 h of incubation. At the end of the treatment, cells were stained with Annexin-V and propidium iodide (PI), in order to determine percentages of viable and dead cells in analyzed samples. Initially applied concentration of H8qasesc on THP-1 cells in the range 1–100 μM induced extremely high apoptotic response (data not shown), thus those data described only the top plateau of the concentration-response sigmoidal curve while ED_{50} concentration could not be calculated. For that reason, concentrations of H8qasesc were decreased for THP-1 cells up to 0.5 μM. As represented in Fig. 2A, most of apoptotic events in the samples treated with 30 and 10 μM were in advanced stages of apoptosis, which means that H8qasesc easily induced cells to execute an apoptotic death. Moreover, percentages of necrotic events were barely above the control levels. Herein, the ED_{50} value was easily calculated and applied in all following experiments on THP-1 cells (Fig. S7, ESI).

View Article Online
DOI: 10.1039/C6MD00199H

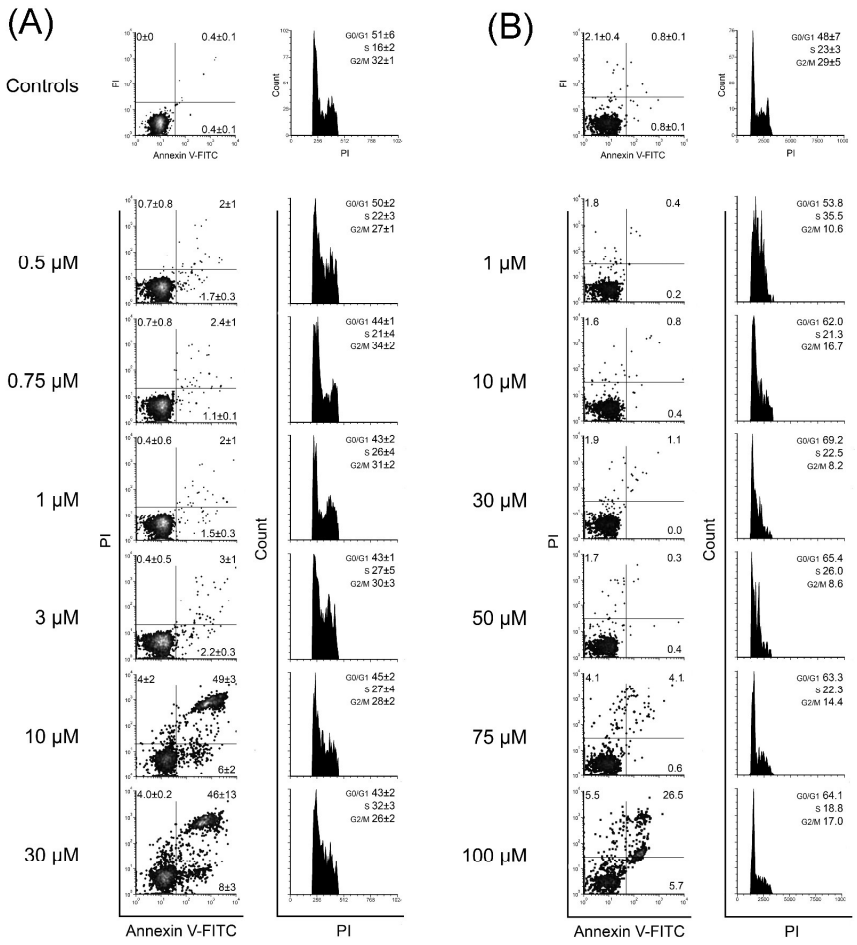

Fig. 2. Activity of H8qasesc on THP-1 cells and AsPC-1 cell lines. Annexin-V and propidium iodide (PI) double staining (left panels) and PI single staining (right panels) of THP-1(**A**) and AsPC-1 (**B**) cells after 24 h treatment with H8qasesc applied in a range of six concentrations. In Annexin-V/PI plots cells are discriminated as viable (non-stained cells, lower left quadrant), cells in early phases of apoptosis (Annexin-V single stained cells, lower right quadrant), cells in late phases of apoptosis (double-stained cells, upper right quadrant), and cells in necrosis (PI single stained cells, upper left quadrant). The same cells evaluated with Annexin-V/PI were fixed in ethanol right after analysis, left overnight and afterwards assayed for distribution within phases of mitotic division with PI single staining method. Frequency of cells found in G0/G1, S and G2/M phases was determined according to non-treated control population. All results are expressed as the mean % ± SD of two replicates from independent experiments for THP-1 cells. Results for AsPC-1 cells are represented as a single replicate considering the second experiment was not performed due to low activity of H8qasesc on this cell line.

View Article Online
DOI: 10.1039/C6MD00199H

Incubation with **1** induced apoptosis as well (Fig. S8A, ESI), with some differences in response of THP1 cells therefore requiring more attention. First, percentages of apoptotic cells were gradually declining with decrease of **1** concentration, but even at 1 μM the incidence of double stained cells was higher compared to those single-stained with Annexin-V. Second, **1** also induced necrotic cell death that exceeded 10% in the samples treated with 100 and 75 μM which was progressively reducing with decrease of applied concentration, but remained persistent and surpassed 1% even at concentration of 1 μM. Such readout indicates on cellular toxicity of investigated compound, and in order to better observe its activity profile we performed additional testing with **1** applied in lower concentrations. In the samples treated with 0.5–3 μM almost the same percentages of cells in necrosis, early and late stages of apoptosis were found (Fig. S8B, ESI). The lack of correlation between applied concentration of **1** and incidence of both types of cell death in treated samples clearly signifies that **1** does not display concentration-dependent activity, but rather intrinsic toxicity. Since these results showed that **1** possess undesirable profile of activity, additional experiment for the second replicate has not been performed. Cisplatin (CDDP) was used as a reference compound, considering it is also the metal complex highly efficient against various types of cancer. In 24 h of incubation on THP-1 cells with a concentration span (1–75 μM), CDDP concentration-dependently induced increase in percentage of cells entering apoptotic death (Figs S7 and S9, ESI). However, contrary to **1**, only a small portion of apoptotic cells were conducted into advanced phases of apoptosis, and as well contrary to **1**, CDDP did not induce significant increase of necrotic events.

Quite the opposite to the effect seen on THP-1 cell line, on AsPC1 cells the ligand H8qasesc induced noteworthy increase of apoptotic events only at the highest applied concentration of 100 μM (Fig. 2B). However, some incidence of cell death was seen in the sample treated with concentration of 75 μM, but those cells were either PI single-stained or double stained, while the percentage of pre-apoptotic events was on the level of non-treated control. It is important to notice that according to control samples, AsPC1 cells contrary to THP-1 cell line spontaneously enter necrosis rather than apoptosis, thus only compound that acts as strong apoptosis inducer would lead AsPC1 cells to advanced stages of apoptotic death. Considering the lack of early apoptotic events, double-stained cells in the sample treated with H8qasesc at 75 μM more probably belonged to necrotic instead of cells in advanced stages of apoptosis,[37] as a result of weak pro-apoptotic stimuli. Contrary, treatment

View Article Online
DOI: 10.1039/C6MD00199H

with H8qasesc at 100 μM has easily driven AsPC-1 cells from the initial to advanced stages of apoptotic death, while percentage of PI single-stained events remained equal to that after treatment with 75 μM. Estimated ED_{50} concentration for H8qasesc was above maximally applied 100 μM, while the same could not be calculated for **1** and CDDP due to their inactivity on AsPC-1 cell line.

2.5. H8qasesc and CDDP induced different alterations in cell cycle distribution

Changes in cell cycle distribution have been evaluated on the same cell populations that were previously analyzed for pro-apoptotic activity of investigated compounds. Considering that **1** showed undesirable activity profile on THP-1 cells and lack of activity on AsPC-1 cell line, distribution within phases of cell cycle division was evaluated on cells treated with H8qasesc on the both cell lines, and CDDP on THP-1 cells. The ligand H8qasesc induced concentration-dependent accumulation of THP-1 cells at the S phase accompanied with reduced percentages of cells at the G0/G1 and G2/M phases (Fig. 2A). CDDP induced accumulation of THP-1 cells at the G2/M in the sample treated with concentration of 1 μM, which turned into accumulation at the S phase in the sample subjected to 3 μM, and then in a concentration-dependent manner gradually slipped at the G0/G1 cell cycle arrest (Fig. S9, ESI). These results indicate that H8qasesc and CDDP exhibit different mechanisms of activity on THP-1 cell line. In AsPC-1 cells H8qasesc stimulated accumulation of cells at the S phase only at the lowest applied concentration, while increase of its concentration arrested the cell division at the G0/G1 phase (Fig. 2B).

2.6. Apoptosis induced by H8qasesc was highly caspase-dependent but without activation of caspase-8 and -9

To determine whether apoptosis induced by H8qasesc and CDDP was driven by caspase-dependent pathway or not, we performed 6 h treatment of THP-1 cells with H8qasesc and CDDP applied at their ED_{50} concentrations, concomitantly incubated or not with pan-caspase inhibitor *N*-benzyloxycarbonyl-Val-Ala-Asp(OMe) fluoromethyl ketone (Z-VAD-fmk). The proper concentration of Z-VAD-fmk (10 μM), not toxic to THP-1 cells, was determined before the experiment. After incubation was ended, treated cells were stained with Annexin-V/PI, and percentage of change in cell death events in Z-VAD-fmk co-treated cells in regard to Z-VAD-fmk non-treated cells was calculated for each labeled feature independently. As it could be seen in Fig. 3, inhibition of caspases activity reduced the both modalities of cell

View Article Online
DOI: 10.1039/C6MD00199H

death induced by H8qasesc and CDDP. It is known that caspases have no role in process of necrotic death, thus reduced percentage of PI single-stained events by Z-VAD-fmk indicates that necrotic cells recorded in Z-VAD-fmk non-treated samples actually originated from cells which initially entered apoptosis. This result signifies that necrosis, although seen in a very small percent in THP-1 cells incubated for 24 h with H8qasesc and CDDP, came out as a result of aponecrosis, that was inhibited by Z-VAD-fmk almost by the same percent in the samples treated with these two compounds. However, impact of co-treatment with Z-VAD-fmk on process of apoptosis induced by H8qasesc and CDDP was quite different. In cells treated with H8qasesc, inhibition of caspases reduced development of early apoptotic events for 66 ± 16%, and 29 ± 1% of double-stained events. On the other hand, Z-VAD-fmk reduced incidence of early apoptosis by 28 ± 4% and 14 ± 6% of those in advanced stages of apoptotic death in CDDP co-treated samples.

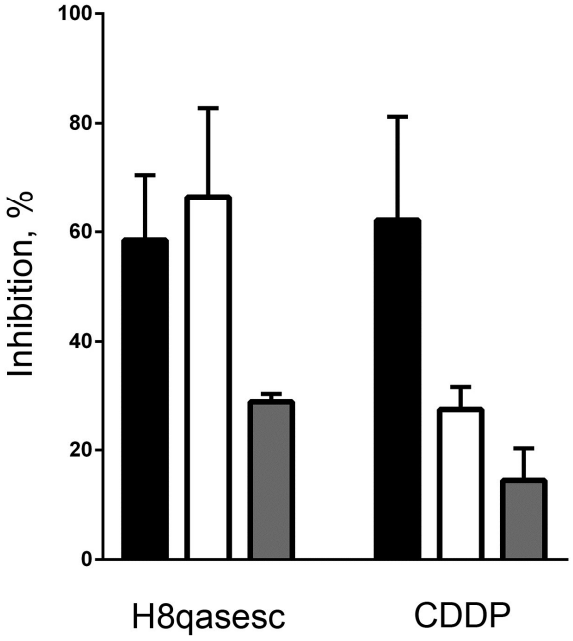

Fig. 3. Role of caspases activity in cell death induced by H8qasesc and CDDP. Percentages of early apoptosis (white bars), advanced apoptosis (gray bars) and necrosis (black bars) inhibition induced by 6 h co-incubation of pancaspase inhibitor Z-VAD-fmk with H8qasesc and CDDP applied in ED_{50} concentrations. Results are expressed as the mean ± SD of two replicates from independent experiments.

View Article Online
DOI: 10.1039/C6MD00199H

The next step was to designate which apoptotic pathway was triggered in THP-1 cells treated with H8qasesc and CDDP. Non-treated controls and cells which underwent treatment with those two compounds applied at their ED_{50} concentration in 6 h were evaluated for caspase-8 and -9 activities. Results of this assay should reveal whether H8qasesc and CDDP initiate apoptosis by activation of extracellular death receptors, or by intrinsic pathway and consecutive activation of caspase-9. There was a low elementary caspase-9 activity found in control samples that points to metabolic or bioenergetics impairments as the underlying cause of spontaneous apoptosis in THP-1 cells (Fig. S10, ESI). Treatment with H8qasesc, however, did not increase activity of caspase-9 compared to non-treated controls, while activity of caspase-8 in H8qasesc-treated cells was below control levels. CDDP also induced discrete alterations in activity of evaluated caspases that may be described as a modest activation of caspase-8 above the level seen in the non-treated control samples.

2.7. H8qasesc can induce CSC reprogramming in AsPC-1 cells

AsPC-1 cells were incubated for 72 h with or without treatment with **1** and H8qasesc applied in concentrations of 1 and 10 μM. Treated and non-treated cells were stained with anti-CD44-FITC and anti-CD133-PE in order to evaluate possible changes in expression of these two most commonly evaluated surface markers on cancer stem cells. According to non-treated samples AsPC-1 cells are displaying $CD44^+/CD133^-$ phenotype, with almost all cells positive for CD44 expression (median fluorescence intensity, MFI = 3173 ± 376). Both compounds induced changes in CD44 expression in treated cells, while expression of CD133 was not affected by either of two tested treatments (Fig. 4). Incubation with **1** and H8qasesc in concentrations of 10 μM, gave almost the same results regarding both percent of $CD44^+$ cells and MFI determined for $CD44^+$ subpopulation (2419 ± 235 in **1** and 2539 ± 185 in H8qasesc-treated cells). However, **1** in concentration of 1 μM induced greater reduction in percent of $CD44^+$ cells, with asymmetrical positively skewed distribution and MFI of 2637 ± 272. It is obvious that although treatment with 1 μM of **1** notably reduced percentage of $CD44^+$ cells, MFI value that represents median density of expressed CD44 per cell was higher in this population compared to the samples treated with 10 μM of **1**. However, the greatest reduction in CD44 expressing cells was achieved by the treatment with H8qasesc at 1 μM. This population of cells was symmetrically distributed with significantly reduced MFI of 1800 ± 93 in $CD44^+$ subpopulation.

View Article Online
DOI: 10.1039/C6MD00199H

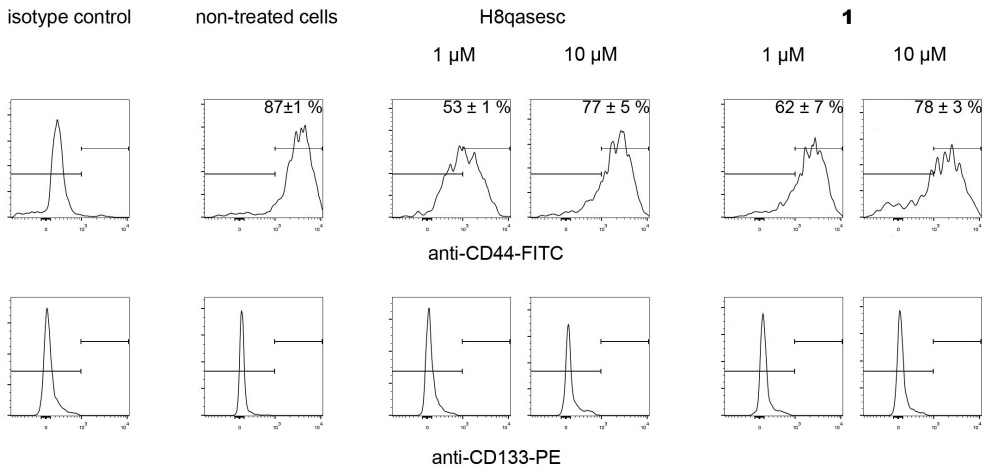

Fig. 4. Pro-differentiation activity of H8qasesc and **1**. Changes in CD-44 expression on AsPC-1 cells after 3-day treatment with H8qasesc and **1** applied in two concentrations. Results are represented as the mean ± SD of two replicates. Treatments did not induce any change in expression of CD-133.

2.8. Plasmid DNA interaction study

The nuclease abilities of H8qasesc and **1** in the absence of any reducing agents were investigated using electrophoretic analysis on pUC19 plasmid incubated with increasing concentrations of investigated compounds. As represented in Fig. 5, electrophoresis of non-treated plasmid pUC19 (lane 1 on both gels) resulted in formation of a strong band of supercoiled DNA (FI) and pale band of nicked plasmid form (FII). Treatment of pUC19 with H8qasesc in the concentration range 0.125–0.875 mM did not induce any variations in neither FI nor FII bands compared to non-treated control. On the other hand, **1** applied already at its lowest concentration of 0.125 mM induced discrete smudging but not accompanied with accelerated intensity of FII form (Fig. 5B, lane 2). Further rise in the concentration of **1** resulted in smear formation together with gradual vanishing of FI form. This result shows that plasmid DNA was massively concentration-dependent degraded by **1**, thus the complex possesses a strong nuclease activity. Also, starting from 0.25 mM of **1** some amount aggregated plasmid DNA has been seen at the edge of the sample well. This aggregation might be explained by the formation of multiple hydrogen bonds between the complex cation of **1** and phosphate moieties of plasmid DNA. The similar interactions were observed

View Article Online
DOI: 10.1039/C6MD00199H

between the complex cation and perchlorate anion in the crystal structure of **1**, since perchlorate anion as a phosphate DNA groups has a tetrahedral geometry. The aggregates were progressively fading away following increase in concentration of **1** most probably as a result of nuclease activity of the complex.

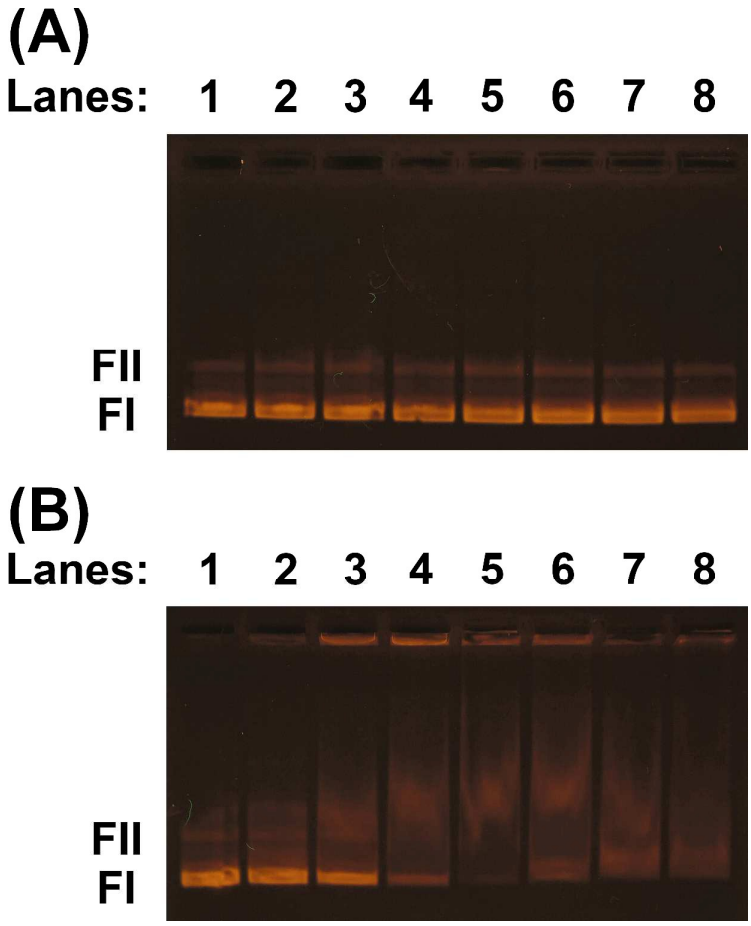

Fig. 5. Agarose gel electrophoresis of interaction of pUC19 with H8qasesc (A) and complex **1** (B). The interactions were investigated by incubation for 90 min of 460 ng plasmid in 20 µL of 40 mM bicarbonate buffer (pH 8.4) at 37 °C, with different concentrations of H8qasesc and **1**. Lane 1 – control plasmid pUC19; lanes 3–8: pUC19 with 0.125, 0. 25, 0.375, 0.5, 0.625, 0.75 and 0.875 mM concentration of H8qasesc (A) and **1** (B).

View Article Online
DOI: 10.1039/C6MD00199H

2.9. Docking studies to DNA and human serum albumin (HSA)

Molecular docking is extremely useful tool in drug discovery to understand the drug–biological target interactions and to investigate the potential binding mode and energy. In our docking study, to examine the binding of the ligand H8qasesc and complex **1** to DNA, the duplex of the sequence $d(CGCGAATTCGCG)_2$ (PDB ID: 3U2N)[38] was used. *In silico* molecular docking experiment revealed that the docked ligand H8qasesc showed absolute preference for minor groove binding (Fig. 6A), with binding energies in the range –27.2 to –29.3 kJ mol^{-1}. No intercalation positions were found. The established interactions between H8qasesc and DNA nucleotides are hydrogen bonds (Fig. 6B). This is expected since H8qasesc consists of groups that are hydrogen bond donors (particularly NH and NH_2 groups), as well as hydrogen bond acceptors (the quinoline nitrogen atom). On the other hand, molecular docking of **1** gave conformations binding to both minor and major groove, with the preference for the major groove (Fig. 6C). Differences between best docking positions in major and minor groove are in the range 0.418–0.836 kJ mol^{-1}. No intercalating structures were found. Interactions of the complex **1** with DNA are similar to those reported for the ligand. Additionally, aromatic systems from the coordinated ligands tend to form CH–π interactions with DNA bases (Fig. 6D).

View Article Online
DOI: 10.1039/C6MD00199H

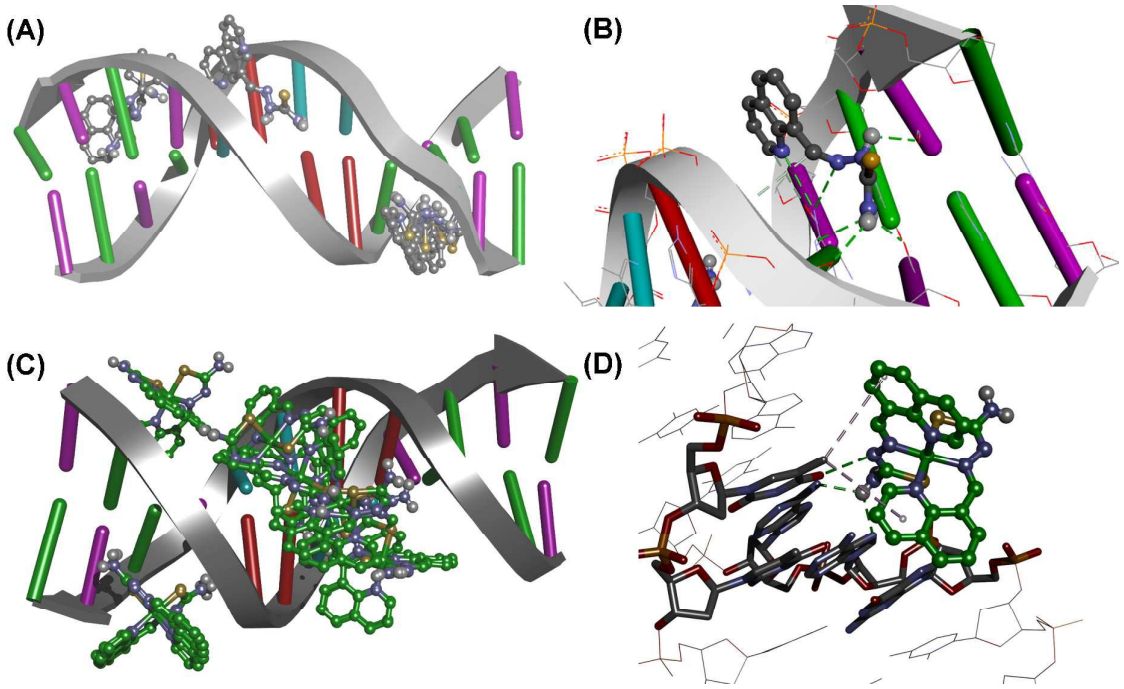

Fig. 6. (A) H8qasesc docking conformations. (B) H8qasesc – minor groove DNA marked interactions. (C) The complex **1** docking conformations. (D) **1** – major groove DNA marked interactions. Dodecamer of the sequence d(CGCGAATTCGCG)$_2$ (PDB ID 3U2N)[38] was used. Color code for interactions: green - hydrogen bonds; grey - aromatic interactions.

HSA is best known for its ligand binding capacity. It provides a repository for an extraordinarily diverse range of molecules which makes it an important factor in the pharmacokinetic behavior of many drugs by affecting their efficiency and rate of delivery.[39] Additionally, the feature of HSA to accumulate in solid tumors raises interest of medicinal chemists to explore ability of newly synthesized compounds to bind to and use HSA as a carrier, and yields the rationale for developing the albumin-based drug delivery systems for tumor targeting drugs.[40] Here we performed a docking analysis protocol to obtain information on H8qasesc and **1** interaction with HSA.

Docking of H8qasesc into HSA showed preference to earlier reported heme binding pocket[41-43] (Fig. S11A, ESI) instead of site II near Trp 214, where **1** is found to bind (Fig. S11B, ESI). Calculated binding energy of –32.6 kJ mol^{-1} suggests significant interaction of the ligand H8qasesc with HSA. Quantified interactions of **1** with amino acid residues in binding site of HSA are given in Table S5 (ESI).

View Article Online
DOI: 10.1039/C6MD00199H

2.10. General discussion

In this work, we report synthesis of novel Co(III) complex with H8qasesc ligand. Both compounds were characterized with single crystal XRD. Structure of **1** in solid state revealed that two molecules of ligand were NNSe tridentately coordinated to Co(III) ion. Every ligand molecule forms one 5-membered and 6-membered chelate ring. NMR studies indicate the same coordination mode in solution.

Although the activity of the ligand on several cancer cell lines was previously investigated, due to differences in applied methodologies it is not possible to compare our current results with the previously published data.[3] While colorimetric MTT assay allows the observation of reduced proliferation rates of treated cells in regard to non-treated ones, it does not provide the insight into reasons why treated cells have been decreased in number, on the other hand, Annexin-V/PI double staining gives direct assessment to the information about the magnitude and type of cell death induced. Currently applied methodological approach also includes information on cell death and cell cycle changes both gained on the very same treated cell population, giving the opportunity for an accurate observation of variations in those two parameters induced by different concentrations of investigated compounds. Therefore, instead to declare for activity of investigated treatments just according to relative number of viable cells in treated samples, we can also review their profiles of activity. CDDP, H8qasesc, and **1**, which we evaluated in the current study, make a perfect trio, considering that each of them illustrates a distinctive mode of anticancer activity.

The CDDP, used here as a reference compound, is nowadays the most efficient metal complex for the treatment of various types of cancer. Even though the Food and Drug Administration does not approve it for the first-line treatment of acute leukemia, laboratory and clinical investigations report its ability to induce apoptosis in leukemia cells and even remission in some aggressive forms of leukemia.[44, 45] Current results show that CDDP concentration-dependently initiated apoptosis in THP-1 cell line, but almost all of the cells persisted in the early phase of apoptotic death at the end of 24 h incubation period. Subsequent cell cycle analysis offered some clues to understand reaction of THP-1 cells to the CDDP treatment. In spite of the fact that CDDP exerts various mechanisms that affect survival of malignant cells, the most important of them is its ability to create DNA lesions.[46-48] The majority of those DNA injuries are intrastrand cross-links which can be bypassed by activation of translesion synthesis polymerases during DNA replication, which are able to

View Article Online
DOI: 10.1039/C6MD00199H

accommodate bulky lesions. On the contrary, interstrand cross-links, which account for a few percentage of CDDP adducts, cannot be bypassed since these cause features such as extrusion of the cytosines of the cross-link sites, bending the helix axis towards the minor groove and large DNA unwinding,[49] whereas their correction involves a complex interplay between a series of DNA repair pathways.[50] According to our results, accumulations of cells at the G2 check point and the S phase found in samples treated with lower concentrations were caused by obstacles during DNA synthesis, but in these samples apoptosis has not been initiated. Starting from the samples treated with CDDP at concentration of 10 μM and higher, there were synchronized appearance of cells at the G1-to-S arrest and early apoptotic events, which percentages were concurrently increasing in a concentration-dependent manner. It is obvious that the cells treated with CDDP in low concentrations were not halted to start DNA replication, although those were passing through the S phase more slowly than non-treated, undamaged cells. CDDP applied in higher concentrations obviously induced DNA damage in extent that was increasing concentration-dependently. Therefore, those cells were arrested by activation of G1-to-S checkpoint, which initiates complex network of repair pathways in order to maintain genomic integrity.[51] Even though it has never been demonstrated, it is logically to expect that the incidence of interstrand cross-links increases with the rise of CDDP concentration on cells. Also, it is not known for how long cells affected by CDDP treatment can idle at the G1-to-S arrest before apoptosis is finally initiated, but our results indicate that CDDP-treated cells, even after exposure of phosphatidylserine, procrastinated the execution phase of apoptotic process for quite some time. All these facts correspond with relatively poor percent of inhibited apoptosis by co-treatment with Z-VAD-fmk accompanied with high percent of inhibited necrosis. The lack of elevated caspase-8 and -9 activities found after 6 h might be due to a short incubation time, but we previously reported that even after 24 h of incubation CDDP did not induce pan-caspase activation in H460 cells.[3]

A successful anticancer agent is expected not only to elicit apoptosis, but to initiate the triggering event(s) that would drive the chains of cascaded actions within a short period of time, leading treated cells throughout the whole process of programmed cell death starting from its initiation, execution, and finally termination. Our results indicate that H8qasesc maybe meets those requirements. Contrary to CDDP, this compound is powerful apoptosis inducer in THP-1 cells, which easily drove them throughout the course of programmed cell death. Although we yet do not have detailed knowledge about the mechanisms of H8qasesc activity on THP-1 cells, regarding the changes in cell cycle progression, H8qasesc also

View Article Online
DOI: 10.1039/C6MD00199H

interferes with the process of DNA synthesis. It is important to notice that the treatment with H8qasesc did not stimulate formation of cell cycle arrest but only extended the time cells spent at the S phase, which means that treated cells most probably did not activate multifaceted repair pathways. This clearly signifies that H8qasesc and CDDP do not share the same mechanism of activity. However, DNA docking analysis revealed that H8qasesc is a minor groove binder with no intercalating properties, while experimental results with pUC19 showed that H8qasesc did not display nuclease activity on plasmid DNA. On the other hand, treatment with H8qasesc also did not stimulate activation of either caspase-8 or -9. However, result provided after co-incubation with pan-caspase inhibitor revealed that apoptosis induced by H8qasesc is highly caspase-dependent, suggesting that some other caspase than caspase-8 or -9 might be responsible for regulation of apoptosis induced by H8qasesc. For that matter, it is very possible that caspase-2 was involved knowing it can be activated due to formation of free radical species, DNA-damage, or cytoskeletal disruption,[52] which should be further investigated. It is important to underline that the results on DNA were either theoretical in the case of docking analysis or gained in *in vitro* model that was depleting regular nuclear DNA milieu. Thus, our results provide information on possible H8qasesc interactions while for the exact conformation of the H8qasesc with his targets, additional experiments on intact cells will be needed. Also, at this point we cannot be sure that H8qasesc does not experience structural alteration(s) due to enzymatic transformation either in serum or in targeted cells. It would be of special importance to determine percentage of HSA occupied by H8qasesc in the human serum, as well as the type of interaction being it irreversible or competitive. Those parameters will be helpful in predicting a possible effect on transport and metabolism of heme that might be induced by the treatment with H8qasesc.

Complexation of H8qasesc with Co has resulted in compound with quite different properties. Already at the first screening on THP-1 cell line it was obvious that **1** displays aggressive mode of activity, inducing necrosis and apoptosis. Its intrinsic toxicity was further confirmed in a range of several times lower concentrations. However, its ED_{50} value computed from one replicate, carried on THP-1 cells, is almost the same as that of H8qasesc, and more importantly it is several times lower compared to ED_{50} achieved by CDDP. Considering that the aim of our investigation was to determine ability of H8qasesc and **1** to induce apoptosis in 24 h with CDDP as a referent compound, H8qasesc and its Co complex might be proclaimed as very successful anticancer agents just relying on ED_{50} concentrations. How actually Pd(II) and Pt(II) complexes increase anticancer potency of H8qasesc, as well as

View Article Online
DOI: 10.1039/C6MD00199H

do those two metals significantly change the favorable mode of H8qasesc activity should be investigated in the next round, but all three metals have in common to drastically reduce the free radical-scavenging activity of H8qasesc.[3] Additionally, we demonstrated that **1** displayed vigorous nuclease activity on plasmid pUC19, completely digesting its DNA in concentration-dependent manner.

Results obtained on THP-1 cell line are representing the baseline evidence on pro-apoptotic activity of investigated compounds. Nevertheless, we were far more curious on how the investigated compounds will affect survival of AsPC-1 cells. As we briefly reviewed above, AsPC-1 cell line is categorized as CSCs. Those are poorly differentiated, fast dividing, self-renewing cells, which sustain the long-term clonal maintenance of the neoplasm. CSCs are highly resistant to pro-apoptotic agents, with unique ability to stop dividing and "hide" into the state of dormancy while escaping the harmful impact of an efficient anti-cancer agent. While neither CDDP nor **1** did induce cell death in AsPC-1 treated cells, H8qasesc generated apoptotic response in its highest applied concentration. More interestingly, only H8qasesc treatment at its lowest concentration induced accumulation of AsPC-1 cells at the S phase, while in all other samples cells were arrested at the G0/G1 phase. Although additional experiments do remain necessary to confirm that AsPC-1 cells are shifted into a dormant state, for example by determining the proportion of cells within G0 phase by lack of cyclin-E expression, the level of probability of dormancy rises with the facts that there was not a significant concentration-dependent variation in the magnitude of the arrest. Therefore, the G0/G1 arrest found in samples treated with H8qasesc already at concentration of 10 μM means that AsPC-1 cells were distressed but successfully resisted to apoptotic stimuli up to the concentration of 100 μM when the pro-apoptotic triggering mechanism became too strong to be ignored.

CD44 is a multifunctional class I transmembrane glycoprotein involved in lymphocyte activation, recirculation and homing, adhesion of extracellular matrix, angiogenesis, and cell proliferation, differentiation, and migration.[53, 54] It is also involved in numerous complex-signaling cascades, while reacting with osteoponin regulates its cellular function leading to tumor progression. Differentiation in breast CSCs by knockdown of CD44 showed dramatically changed gene expression pattern in treated cells compared to original cells.[55] Hong et al demonstrated that $CD44^+$ cells are responsible for the resistance to gemcitabine in pancreatic cancer.[56] The same authors reported on positive correlation between CD44 expression with histological grade and poor prognosis. All these facts clearly

View Article Online
DOI: 10.1039/C6MD00199H

demonstrate the significance of CD44 down expression in AsPC-1 cells. Our results revealed that 3-day incubation with **1** achieved percentage of $CD44^+$ cells, but in the same time average expression of CD44 receptors per cell in $CD44^+$ subpopulation was not remarkably reduced. This implies that remaining $CD44^+$ cells retained their phenotypic character. Quite contrary, treatment with H8qasesc in lower tested concentration successfully reduced percentage of $CD44^+$ cells together with strikingly decreased expression of targeted protein on the membranes of $CD44^+$ subpopulation.

3. CONCLUSION

Activity of H8qasesc on two diverse cell lines demonstrated ligand's ability to induce apoptotic death in more than a half treated non-CSC cells already at concentration of 10 μM. This apoptotic response was shown to be highly caspase-dependent, but did not include activation of either caspase-8 or -9. In CSC model, treatment with H8qasesc at 100 μM triggered apoptosis in a highly resistant AsPC-1 cell line, while at low concentration the ligand successfully caused the change in their phenotype. Our results clearly indicate that with dose titration of H8qasesc it can be expected to achieve apoptotic death of non-CSC and CSC, or CSC differentiation, which would make them more vulnerable to pro-apoptotic drugs. In spite of our expectations, complexation of H8qasesc with Co(III) did not result in a compound with outstanding properties. The complex **1** displayed strong, but toxic response on THP-1 cell line with lack of ability to trigger death in CSCs. Its vigorous nuclease activity may be the relying cause of high incidence of necrosis seen in the treated samples. Finally, the excellent activity profile of H8qasesc reviewed herein deserves its further evaluation in terms of antineoplastic agent with expanded spectrum of actions.

ACKNOWLEDGMENTS

The authors acknowledge networking support by the COST Action CM1106 StemChem – "Chemical Approaches to Targeting Drug Resistance in Cancer Stem Cells". The work was founded by the Ministry of Education, Science and Technological Development of the Republic of Serbia (Grant 172055).

View Article Online
DOI: 10.1039/C6MD00199H

REFERENCES

1. C. Pizzo, P. Faral-Tello, G. Salinas, M. Flo, C. Robello, P. Wipf and S. G. Mahler, *Medchemcomm*, 2012, **3**, 362-368.
2. H. G. Mautner, W. D. Kumler, Y. Okano and R. Pratt, *Antibiot. Chemother. (Northfield)*, 1956, **6**, 51-55.
3. N. Filipovic, N. Polovic, B. Raskovic, S. Misirlic-Dencic, M. Dulovic, M. Savic, M. Niksic, D. Mitic, K. Andelkovic and T. Todorovic, *Monatsh. Chem.*, 2014, **145**, 1089-1099.
4. T. R. Todorovic, A. Bacchi, D. M. Sladic, N. M. Todorovic, T. T. Bozic, D. D. Radanovic, N. R. Filipovic, G. Pelizzi and K. K. Andelkovic, *Inorg. Chim. Acta*, 2009, **362**, 3813-3820.
5. M. D. Revenko, V. I. Prisacari, A. V. Dizdari, E. F. Stratulat, I. D. Corja and L. M. Proca, *Pharm. Chem. J.*, 2011, **45**, 351-354.
6. K. Bednarz, *Diss. Pharm.*, 1958, **10**, 93-98.
7. U.S. Patent 4665173 A, 1987.
8. D. L. Klayman, J. P. Scovill, J. F. Bartosevich and J. Bruce, *Journal of Medicinal Chemistry*, 1983, **26**, 35-39.
9. D. L. Klayman, J. P. Scovill, J. F. Bartosevich and C. J. Mason, *Eur. J. Med. Chem.*, 1981, **16**, 317-320.
10. 4,657,903, 1987.
11. K. C. Agrawal, B. A. Booth, R. L. Michaud, E. C. Moore and A. C. Sartorelli, *Biochem. Pharmacol. (Amsterdam, Neth.)*, 1974, **23**, 2421-2429.
12. V. Zaharia, A. Ignat, B. Ngameni, V. Kuete, M. L. Moungang, C. N. Fokunang, M. Vasilescu, N. Palibroda, C. Cristea, L. Silaghi-Dumitrescu and B. T. Ngadjui, *Med. Chem. Res.*, 2013, **22**, 5670-5679.
13. M. Liu, P. L. Xu and Z. J. Wang, *Yao Xue Xue Bao*, 1992, **27**, 388-393.
14. V. Calcatierra, O. Lopez, J. G. Fernandez-Bolanos, G. B. Plata and J. M. Padron, *Eur. J. Med. Chem.*, 2015, **94**, 63-72.
15. D. L. Klayman, J. P. Scovill, C. J. Mason, J. F. Bartosevich, J. Bruce and A. J. Lin, *Arzneimittelforschung*, 1983, **33**, 909-912.
16. M. Zec, T. Srdic-Rajic, A. Konic-Ristic, T. Todorovic, K. Andjelkovic, I. Filipovic-Ljeskovic and S. Radulovic, *Anticancer Agents Med. Chem.*, 2012, **12**, 1071-1080.

View Article Online
DOI: 10.1039/C6MD00199H

17. T. Srdic-Rajic, M. Zec, T. Todorovic, K. Andelkovic and S. Radulovic, *Eur. J. Med. Chem.*, 2011, **46**, 3734-3747.
18. M. Zec, T. Srdic-Rajic, A. Krivokuca, R. Jankovic, T. Todorovic, K. Andelkovic and S. Radulovic, *Med. Chem.*, 2014, **10**, 759-771.
19. S. Bjelogrlic, T. Todorovic, A. Bacchi, M. Zec, D. Sladic, T. Srdic-Rajic, D. Radanovic, S. Radulovic, G. Pelizzi and K. Andelkovic, *J. Inorg. Biochem.*, 2010, **104**, 673-682.
20. N. Gligorijevic, T. Todorovic, S. Radulovic, D. Sladic, N. Filipovic, D. Godevac, D. Jeremic and K. Andelkovic, *Eur. J. Med. Chem.*, 2009, **44**, 1623-1629.
21. A. Molter, G. N. KaluÄ‘eroviÄ‡, H. Kommera, R. Paschke, T. Langer, R. PÃ¶ttgen and F. Mohr, *J. Organomet. Chem.*, 2012, **701**, 80-86.
22. C. R. Kowol, R. Eichinger, M. A. Jakupec, M. Galanski, V. B. Arion and B. K. Keppler, *J. Inorg. Biochem.*, 2007, **101**, 1946-1957.
23. H. Shen, H. Zhu, M. Song, Y. Tian, Y. Huang, H. Zheng, R. Cao, J. Lin, Z. Bi and W. Zhong, *BMC Cancer*, 2014, **14**, 629.
24. A. Molter, J. Rust, C. W. Lehmann, G. Deepa, P. Chiba and F. Mohr, *Dalton Transactions*, 2011, **40**, 9810-9820.
25. Y. K. Bhoon, J. P. Scovill and D. L. Klayman, *Indian J. Chem.*, 1983, **22A**, 267-269.
26. N. R. Filipovic, S. Bjelogrlic, A. Marinkovic, T. Z. Verbic, I. N. Cvijetic, M. Sencanski, M. Rodic, M. Vujcic, D. Sladic, Z. Strikovic, T. R. Todorovic and C. D. Muller, *RSC Adv.*, 2015, **5**, 95191-95211.
27. Z. Al-Eisawi, C. Stefani, P. J. Jansson, A. Arvind, P. C. Sharpe, M. T. Basha, G. M. Iskander, N. Kumar, Z. Kovacevic, D. J. Lane, S. Sahni, P. V. Bernhardt, D. R. Richardson and D. S. Kalinowski, *Journal of Medicinal Chemistry*, 2016, **59**, 294-312.
28. V. Cracan and R. Banerjee, in *Metallomics and the Cell*, ed. L. Banci, Springer Netherlands, Dordrecht, 2013, pp. 333-374.
29. R. G. Matthews, *Met. Ions Life Sci.*, 2009, **6**, 53-114.
30. N. Filipovic, S. Grubisic, M. Jovanovic, M. Dulovic, I. Markovic, O. Klisuric, A. Marinkovic, D. Mitic, K. Andelkovic and T. Todorovic, *Chem. Biol. Drug Des.*, 2014, **84**, 333-341.

View Article Online
DOI: 10.1039/C6MD00199H

31. S. A. Mani, W. Guo, M. J. Liao, E. N. Eaton, A. Ayyanan, A. Y. Zhou, M. Brooks, F. Reinhard, C. C. Zhang, M. Shipitsin, L. L. Campbell, K. Polyak, C. Brisken, J. Yang and R. A. Weinberg, *Cell*, 2008, **133**, 704-715.
32. B. Beck and C. Blanpain, *Nat. Rev. Cancer*, 2013, **13**, 727-738.
33. R. Manikandan, P. Viswanathamurthi, K. Velmurugan, R. Nandhakumar, T. Hashimoto and A. Endo, *J. Photochem. Photobiol., B*, 2014, **130**, 205-216.
34. F. H. Allen, *Acta Crystallogr., Sect. B: Struct. Sci.*, 2002, **58**, 380-388.
35. M. T. Zimmerman, C. A. Bayse, R. R. Ramoutar and J. L. Brumaghim, *J. Inorg. Biochem.*, 2015, **145**, 30-40.
36. R. L. Prior, X. L. Wu and K. Schaich, *J. Agric. Food Chem.*, 2005, **53**, 4290-4302.
37. D. V. Krysko, T. Vanden Berghe, K. D'Herde and P. Vandenabeele, *Methods*, 2008, **44**, 205-221.
38. D. G. Wei, W. D. Wilson and S. Neidle, *J. Am. Chem. Soc.*, 2013, **135**, 1369-1377.
39. M. Fasano, S. Curry, E. Terreno, M. Galliano, G. Fanali, P. Narciso, S. Notari and P. Ascenzi, *IUBMB Life*, 2005, **57**, 787-796.
40. F. Kratz, *J Control Release*, 2008, **132**, 171-183.
41. M. Wardell, Z. M. Wang, J. X. Ho, J. Robert, F. Ruker, J. Ruble and D. C. Carter, *Biochem. Biophys. Res. Commun.*, 2002, **291**, 813-819.
42. P. A. Zunszain, J. Ghuman, T. Komatsu, E. Tsuchida and S. Curry, *BMC Struct Biol*, 2003, **3**, 6.
43. E. Tsuchida, K. Sou, A. Nakagawa, H. Sakai, T. Komatsu and K. Kobayashi, *Bioconjug Chem*, 2009, **20**, 1419-1440.
44. M. Previati, I. Lanzoni, E. Corbacella, S. Magosso, V. Guaran, A. Martini and S. Capitani, *Int J Mol Med*, 2006, **18**, 511-516.
45. J. LaPorte, L. Morris and J. Koepke, *Case Rep Hematol*, 2015, **2015**, 715615.
46. R. Marullo, E. Werner, N. Degtyareva, B. Moore, G. Altavilla, S. S. Ramalingam and P. W. Doetsch, *PLoS One*, 2013, **8**, e81162.
47. A. M. Florea and D. Busselberg, *Cancers (Basel)*, 2011, **3**, 1351-1371.
48. K. Wozniak and J. Blasiak, *Acta Biochim Pol*, 2002, **49**, 583-596.
49. J. M. Malinge, M. J. Giraud-Panis and M. Leng, *J Inorg Biochem*, 1999, **77**, 23-29.
50. J. M. Wagner and L. M. Karnitz, *Mol Pharmacol*, 2009, **76**, 208-214.
51. T. Helleday, E. Petermann, C. Lundin, B. Hodgson and R. A. Sharma, *Nat Rev Cancer*, 2008, **8**, 193-204.

View Article Online
DOI: 10.1039/C6MD00199H

52. J. Puccini, L. Dorstyn and S. Kumar, *Cell Death Differ*, 2013, **20**, 1133-1139.
53. A. Jaggupilli and E. Elkord, *Clin Dev Immunol*, 2012, **2012**, 708036.
54. S. B. Keysar and A. Jimeno, *Mol Cancer Ther*, 2010, **9**, 2450-2457.
55. P. V. Pham, N. L. Phan, N. T. Nguyen, N. H. Truong, T. T. Duong, D. V. Le, K. D. Truong and N. K. Phan, *J Transl Med*, 2011, **9**, 209.
56. S. P. Hong, J. Wen, S. Bang, S. Park and S. Y. Song, *Int J Cancer*, 2009, **125**, 2323-2331.

View Article Online
DOI: 10.1039/C6MD00199H

Graphical abstract and synopsis

Selenosemicarbazone ligand and its Co(III)-based complex were characterized by X-ray analysis. Apoptosis triggered by the ligand was highly caspase-dependent. The ligand initiated reprogramming of cancer stem cells phenotype in AsPC-1 cell line. The complex concentration-dependently digested plasmid DNA which might be the cause of its cytotoxic activity.